Effects of Tip Clearance on the Performance and the Flow Field of a High Rotational Speed Centrifugal Fan

S. Khelladi, sofiane.khelladi@paris.ensam.fr
R. Noguera
S. Kouidri
F. Bakir
R. Rey
Ecole Nationale Supérieure d'Arts et Métiers, Laboratoire d'Energétique et de Mécanique des Fluides Interne, 151 boulevard de l'Hôpital 75013 Paris, FRANCE

R. Cao
College of Energy and Power Engineering, Nanjing University of Aeronautics and Astronautics, Nanjing, 210016 Jiangsu, CHINA

Abstract. A centrifugal fan with high speed and compact dimension was chosen to be studied numerically and experimentally in this paper. The fan studied consists of a shrouded impeller rotating at 34,000 rpm with a small tip clearance 0.7 mm to the fixed outer casing. For the numerical simulation, two computational models with/without tip clearance were set up and the $k - \omega$ SST (Shear Stress Transport) turbulence model and hybrid mesh were applied in the numerical simulation for the unsteady solutions. The overall performance and the major flow features in each component inside a centrifugal fan have been numerically investigated. Together with a series of measurements carried out on a test bench, the static pressure was measured respectively at the sections of impeller inlet and fan outlet, and the mass flow rate was obtained by an orifice plate system. The flow restriction for the centrifugal fan system was obtained and demonstrated to be highly correlated with tip clearance. In presence of the tip clearance, due to the difference of static pressure between the leading and trailing edges of clearance, i.e., the leading and trailing edges of impeller, a strong return flow occurs in the clearance and re-circulates to the main stream inside the impeller passage with a strong flow interaction, inducing the total pressure loss and increasing the flow restriction of the fan system.

Keywords: Centrifugal fan, numerical simulation, measurement, flow field, loss

1. Introduction

As a kind of turbomachinery, the centrifugal fans have been widely adopted by public facilities and electronic industries, due to their large capacity of mass flow and the size compactness. A review clearly clarified the state-of-the-arts of the potential development in the field of centrifugal turbomachinery [1]. It was pointed out that many machines having moderate efficiency are still in operation and could certainly be improved by making use of today's knowledge. The shrouded impellers are usually used in high-specific-speed-type centrifugal fans. Due to the matters that operate, there always exists a tip clearance between the shrouded impeller and outer casing. Therefore, the leakage flow through the tip becomes unavoidable. The impellers of centrifugal fan are linked downstream by vaned diffuser, cross-over bend, and return channel. The main task of the vaned diffuser is to transform as much as possible kinetic energy, available at the impeller exit, into static pressure rise. The main purpose of the return channel is to take out the swirl while guiding the flow to the downstream duct. However, the return channel typically joins the exit from the first stage of a centrifugal machine to the downstream components. For such a kind of turbomachinery, the natures of flow physics involving tip clearance in the impeller and impeller-diffuser vane interaction are inherently becoming two major concerns of research. Nowadays, there are a great deal of studies concerning the effects of impeller-diffuser interaction on flow field and performance. It is shown that there always exists flow separation regime near the diffuser hub extending further downstream [2]. The flow is strongly three-dimensional with secondary flows on hub and shroud of the de-swirl vanes and significant separation downstream of the cross-over bend [3, 4]. Subsequently the flow is not really axisymmetric and that the cross-over bend needs 50% area increased to allow for boundary layer blockage. There is a lot of variance in loss data in this kind of bend, which must be due to unknown variables affecting the results [5]. In presence of the tip clearance in the centrifugal fan, many researches have been shown that the tip clearance plays an important role in the flow field [6] and the leakage flow becomes major source of performance loss and efficiency drop for small sized compressor impellers [7] and how to control the tip leakage flow tends to be more attractive [6].

The development of powerful numerical algorithm and robust commercial tools enable to understand deeply into the unsteady flow field and the mechanisms of loss generation. From the optimized deign points of view, the advanced CFD tools make the optimized design of centrifugal fan possible [8, 9, 10]. The three-dimensional unsteady viscous flow solution was numerically obtained by means of powerful computational facilities and robust software together with very consumptive calculation time [3]. It is common well-known, despite the knowledge accumulated over the past few

decades on the mechanisms of air delivery system, the exact prediction of such flow field by numerical means is still difficult partly due to our inability to model the turbulent viscous flow and the complicated nature of flow through such machines [11, 12]. Still, there were significant differences between computations and experiment, mainly in the wide prediction of the extent of the separation after the bend. This flow is very complex with separations and possibly non-axisymmetry having an effect on downstream components.

Most recently, for the purpose of simplicity, a criterion to define cross-flow fan design parameters was reported [13] according to the most significant variables defining the geometry and then affecting performance and efficiency. This choice of parameters has proved to be effective in a systematic series of experimental tests aimed at investigating directions for design improvement. The aim is to find which are the parameters most affecting fan performances and the effects of their design choice. Indications are found to design fans according to the desired objectives, such as maximum total pressure, total efficiency, and flow rate [14, 15]. The studies about the mechanisms of flow loss generation of centrifugal fans are not well documented yet. However, the energy loss correlation with experimental data was made to show some effective ways in understanding theoretically about the performance and efficiency curves of centrifugal fans [15]. In this paper, a motor-fan utilized in vacuum cleaner was adopted in this study. The centrifugal fan features with its high specific speed and compact size and a tip clearance between the shrouded impeller and outer casing. The numerical model was presented in calculating the flow field with/without tip clearance. In addition with some test work, the comparisons of both the overall performance and flow field were made. The major flow features in each component inside a centrifugal fan have been numerically investigated. The loss generation and the flow restrictions under circumstances of with/without tip clearances were also analyzed.

2. Numerical approach and test rig

2.1 Physical Model

The motor-fan we studied was used to provide large depression capability required by a vacuum cleaner. A shaft is used to connect the centrifugal impeller and motor. Due to the irregular and complex structures in the motor, it is difficult to simulate the flow field combined with the real motor components. Apart from the investigation of flow around the motor structure, the flow through the fan itself is the main concern of research. Therefore, some assumptions are necessary. As shown in figure (1), the centrifugal fan studied consists of the following components: centrifugal impeller, diffuser and return channel. The diffuser with 17 vanes and the return channel with 8 irregular guide vanes enable to de-swirl the flow. An inlet and outlet ducts are imposed to the numerical model to ensure uniform boundary conditions. In order to better understand the effect of tip clearance on overall performance and flow structure, a computational model without the tip clearance was configured (Case I), whilst for the real prototype at practical operating condition, there always exists a tip clearance between the rotating shrouded impeller and the stationary outer casing (Case II). The geometrical and operating parameters of the centrifugal fan are listed in Tables 1 and 2.

Head, H (m)	1300
Flow rate, Qv (m^3/s)	35×10^{-3}
Rotational speed, N (rpm)	34000
Specific speed $N_s = N\sqrt{Q_v}/H^{3/4}$	29

Table 1. Aerodynamic characteristics at operating point

Description	Impeller	Diffuser	Return channel
Radius of blade inlet (mm)	18	52.7	60
Span of the blade at the entry (mm)	13	6.48	11
Inlet blade angle (ř)	64	85	74
Inclination Angle of the blade inlet (ř)	85.8	0	0
Radius of blade exit (mm)	52	66.1	33
Span of the blade at the exit (mm)	5.4	8.43	12
Angle of blade exit (ř)	64	71.6	15
Inclination angle of the blade exit (ř)	0	0	0
Blade number	9	17	8
Blade thickness (mm)	0.8	0.9	1.6

Table 2. Basic geometrical specifications of the centrifugal fan
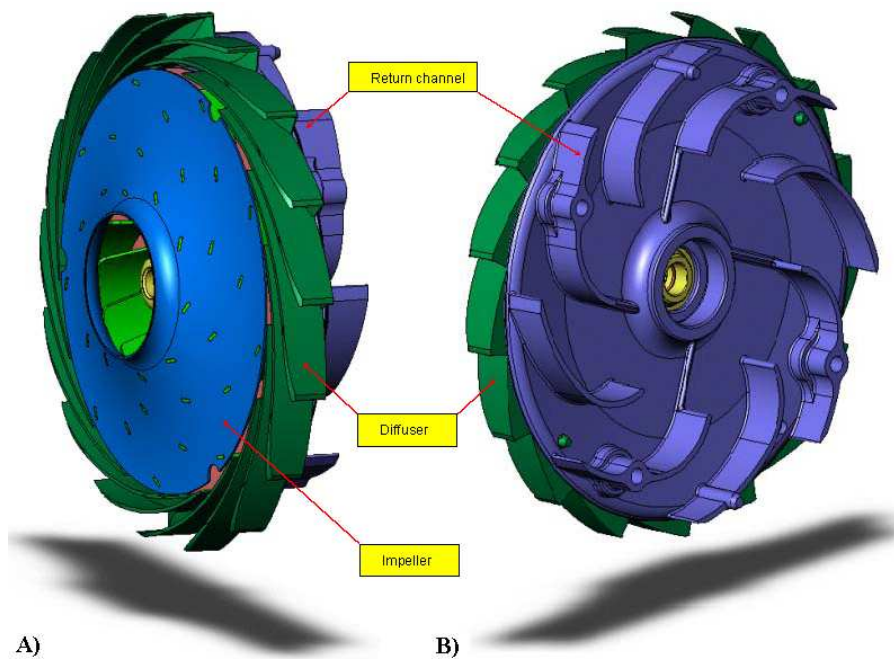
Figure 1. Description of centrifugal fan system, A) front view, B) back view

2.2 Numerical Model

The numerical simulations have been carried out with a code that is based on the finite volume numerical method using the commercial code Fluent 6.1 [16] to solve the full 3D Reynolds Average Navier-Stokes equations. A centered SIMPLE algorithm is used for the pressure-velocity coupling and a second-order upwind discretization is used for the convection and diffusion terms. The unsteady terms are implicit discretized with second-order accuracy. The velocity is specified at the inlet surface for the inlet duct volume and the static pressure is imposed at the exit surface for the outlet duct. Nevertheless, the guide vanes in the return channel are featured as azimuth asymmetry as shown in figure 1. The ratio of the number of impeller blade over the number of diffuser is uneven. Therefore, for an unsteady solution, the computational domain covering all the flow passages is necessary. In order to reduce the grid number but better approximate the near-wall viscous characteristics, the $k - \omega$ SST (Shear Stress Transport) model was then adopted. The treatment close to the wall combining a correction for high and low Reynolds number is available to predict separation on smooth surfaces [17]. Typically, this model gives a realistic estimation of the generation of the turbulent kinetic energy at the stagnation points. The SST model performance has been studied in a large number of cases. In a NASA Technical Memorandum [18], the SST model was rated the most accurate model for aerodynamic applications. As the geometry of the fan is complex, a hybrid mesh is used: tetrahedral for the impeller and the diffuser - return channel volumes, hexahedral for upstream and downstream fluid volumes. A previous study of Khelladi et al [3] shows that a grid of 4.4×10^6 meshes is considered to be sufficiently reliable to make the numerical modeling results independent to the mesh size.

2.3 Measurement Methodology

The measurements of fan characteristics were carried out on a test bench (as shown in Figure 2). The test rig includes an airtight box (0.6m x 0.6m x 0.6m) where the centrifugal fan is placed up and an orifice plate is open at the side wall ensuring a changeable air flow rate from 12 to 60 l/s by changing the diameter of the orifice plate. The Kulite dynamic sensors, with a diameter of 1.6 mm and a band-width of 125 kHz were used to measure the static pressure at the impeller inlet and the return channel outlet. The discrete data were then time-averaged to obtain the steady one. The uncertainty error for static pressure measurement is about ±2.5 mbar which is equivalent to ±0.4 l/s.

3. Results and analysis

4. Overall Performance and Flow Field Description

As shown in figure 3, as a function of air flow, the comparison of the static pressure difference between the predictions with/without tip clearances and the experimental data is presented. The curve with filled square is the calculated one without tip clearance, whilst the one with cross symbols is that for tip clearance, and the discrete circular points are that for
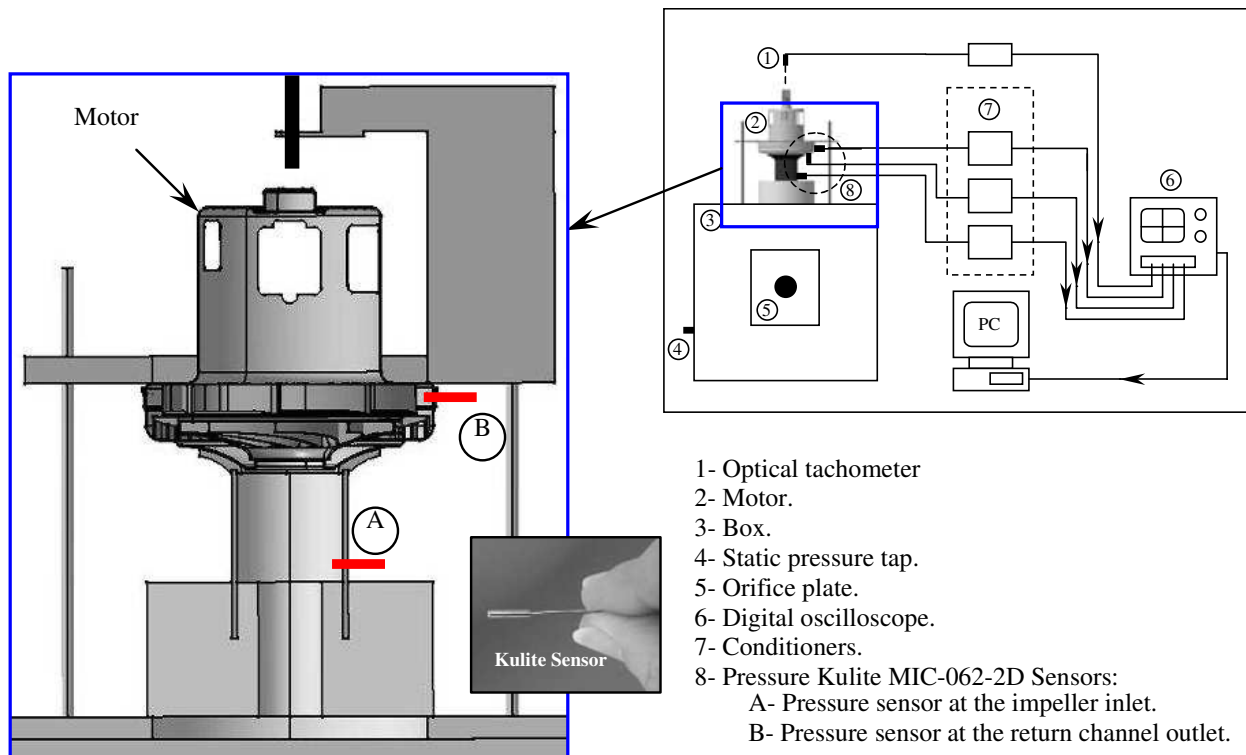
Figure 2. Schematic of the test rig for fan

measurement. It is shown that the calculated curves are in a good tendency with the experimental data, but the predicted curve for the case II agrees much more with the experiment. At the design point of volume flow rate of 0.035 m^3/s which is equivalent to 35 l/s, the errors of static pressure difference with the one measured can then be assessed to be at a level of 41.75% and 3.33% for the case without (Case I) and with (Case II) tip clearances, respectively. It is therefore manifest that the numerical model with the clearance is in adequate accuracy with the measurement. In other words, one can find that the effect of tip clearance on the overall performance can not be ignored.

A blade-to-blade section was selected with 5 mm away from the impeller hub. The sectional view of the static pressure at the section of blade-to-blade at middle radial span is shown in figure 4A) and figure 4B) for the Case I and II, respectively. The static pressure difference between the impeller inlet and diffuser outlet can be roughly assessed which one can find the one for Case I is about twice of the Case II. This implies that the existence of tip clearance reduces the capability of static pressure rise. The inflow condition of downstream component diffuser depends on the flow field at impeller exit. Referring to both cases, it can be found that the flow around one of diffusers is characterized by the fact that the incidence angle is too positive introducing a strong stagnation point at the pressure side near the leading edge, in turn, produce an acceleration regime in the opposite side. Naturally, this kind of flow increases both the static loading of the diffuser and the force fluctuation due to impeller/diffuser interaction. Not only the through flow capability but also the overall performance will be degraded due to the flow blockage existed in the diffuser.
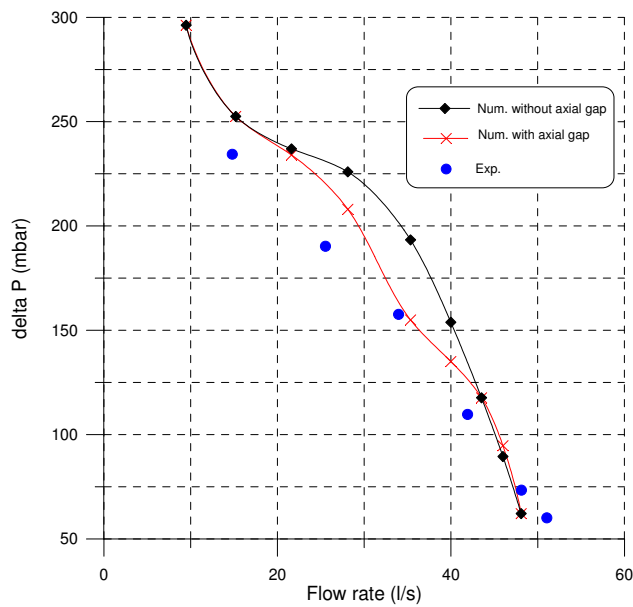
Figure 3. Comparison of overall performance between calculation and measurement
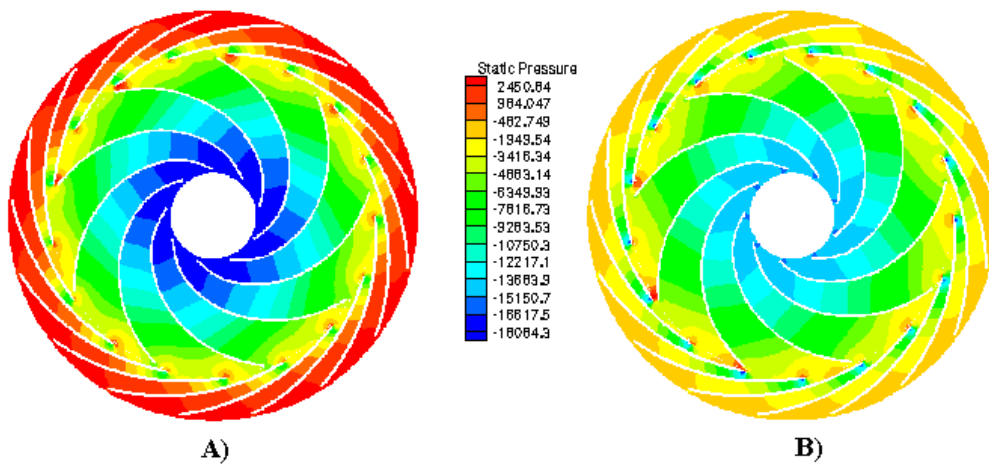
Figure 4. Comparison of contour of static pressure at a blade-to-blade section of mid radial span for the case, A) without tip clearance and B) with tip clearance

The cross-rotating-axis section means the section plotted across the rotating axis. The comparison of the static pressure at the cross-rotating-axis section for the case with/without tip clearance is presented in figure 5, figure 5A) and figure 5B) are for Case I and Case II, respectively. The static pressure through the fan inlet and outlet can be roughly figured out for both cases, for Case I it is about 1.3 times bigger than that of Case II. The static pressure is gradually increased from impeller inlet to outlet, inducing a returned flow inside the tip clearance from the outlet side of impeller back to the inlet and generating a re-circulation flow pattern [3]. As can be seen in figure 5B), the static pressure inside the tip clearance almost keeps constant. In vicinity of impeller inlet, the static pressure of tip clearance is bigger than that of impeller, which produces a source for flow re-circulation and flow distortion ahead of the impeller as well as flow loss generation.
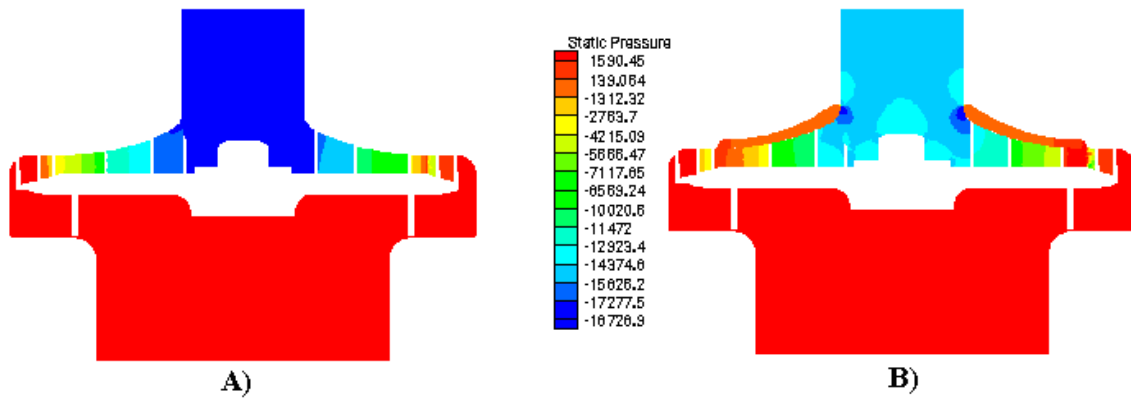
Figure 5. Comparison of contour of static pressure at a cross-rotating-axis section for the case, A) without tip clearance and B) with tip clearance

The comparison of the total pressure at the cross-rotating-axis section is given in figure 6. The maximum total pressure rise for Case I has roughly 2 times of that for Case II. For Case I, the total pressure is uniformly increased through impeller and diffuser but high distortions are found at the cross-over bend and return channel. Whilst for Case II, a non-uniformity exists at impeller inlet and cross-over bend and return channel. The almost constant total pressure inside the tip clearance is found thereafter to generate a stagnation point near the impeller inlet. As mentioned-above, the cross-over bend and return channel are two dominant components with high loss generation.
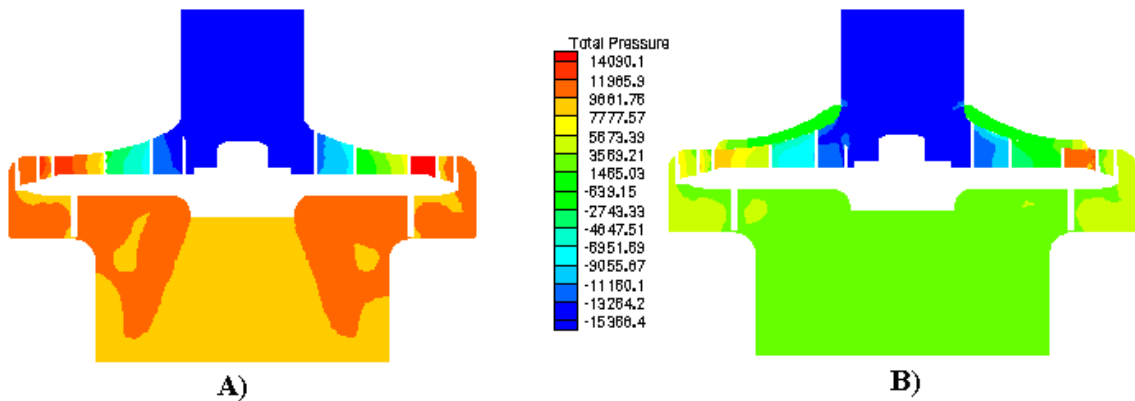
Figure 6. Comparison of contour of total pressure at a cross-rotating-axis section for the case, A) without tip clearance and B) with tip clearance

Figure 7 shows the solution of entropy for both cases in which one can quantitatively understand the loss distribution. For Case I as shown in figure 7A), very high entropy gradients occur through impeller exit, cross-over bend and return channel. This can also be found in figure 7B) for Case II, typically, a big jump appears at the impeller inlet nearby the tip clearance where a strong stagnation point is produced. Due to the high rotating speed, the absolute velocity at impeller exit is so high that a strong swirling flow occurs at the cross-over bend. Due to the narrow frontal area at the cross-over bend and return channel, the strong flow blockage and vortex is accumulated.
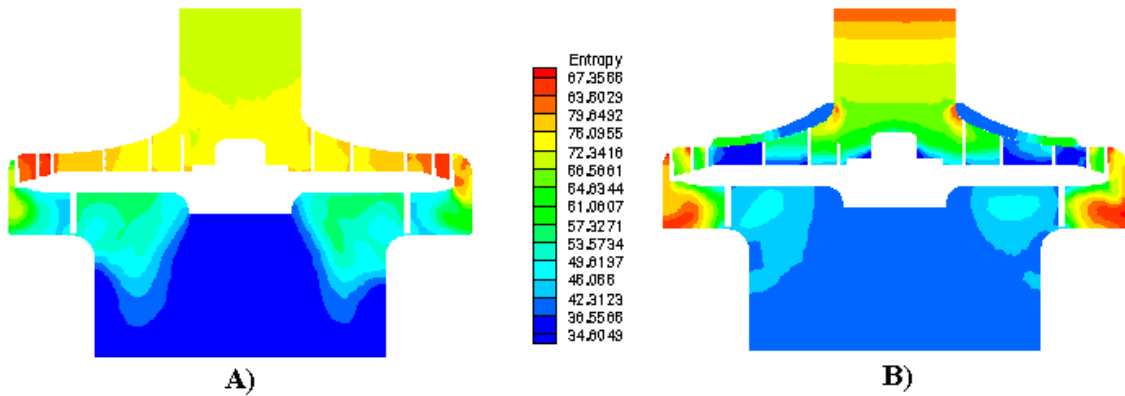
Figure 7. Comparison of contour of entropy at a cross-rotating-axis section for the case, A) without tip clearance and B) with tip clearance

4.1 Loss Generation

In order to easily quantify the loss generation for each flow component, the half view of the flow components for the centrifugal fan system is schematically plotted as shown in figure 8. For the numerical model, an inlet duct and a downstream duct are imposed at fan inlet and outlet for uniform boundary condition specifications. Following is named as A region where the flow comes from inlet duct to the impeller. Through the impeller, the diffuser component is designated as B region. The flow with 90 degree return through the cross-over bend is named as C region. D region is the return channel where guide vanes are installed to suppress strong swirl flow. The outlet duct is represented as E region.
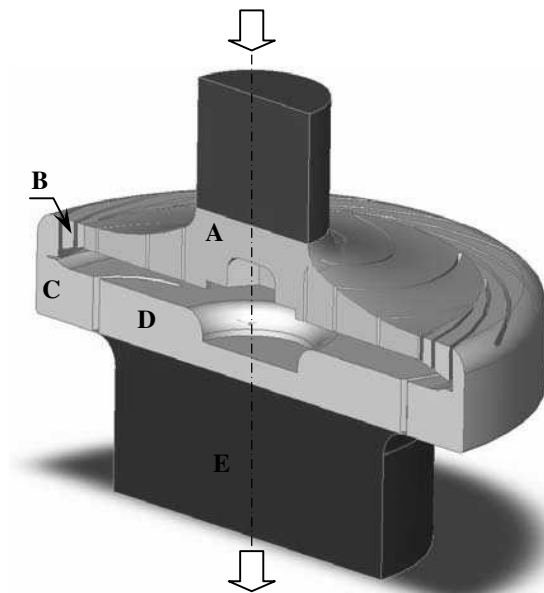
Figure 8. Schematic of the calculation domain with the flow components of the centrifugal fan (half view)

The vorticity amplitude for each component is normalized by that of impeller. As shown in figure 9 (Case I), the maximum vorticity amplitude occurs at the impeller due to its high rotating speed. A, B and C regions have equivalent ones with about half of that of impeller where implies that strong swirling flow occurs that will probably introduce flow blockages and total pressure drop.

Some definitions are chosen for analysis. The static pressure rise coefficient for the stationary compartment can be written as

$$C_p = \frac{P_{s2} - P_{s1}}{P_{t1} - P_{s1}} \tag{1}$$
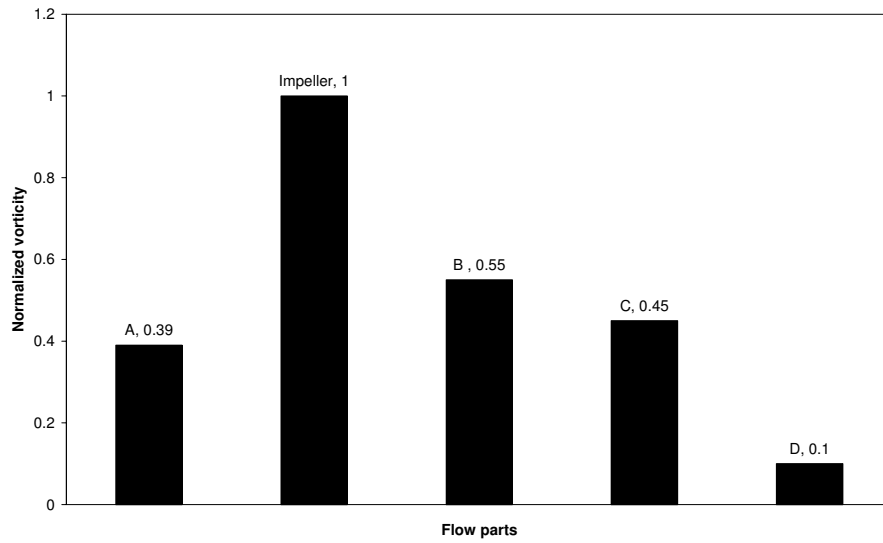
Figure 9. Distribution of normalized vorticity amplitude along the centrifugal fan (Case I)

Where subscript s denotes static pressure, t denotes the total pressure, 2 means the exit section of the component, and 1 is the inlet section of the component. For stationary part, the static pressure recovery coefficient means the capability of static pressure rise through the stationary parts. The static pressure recovery coefficient along the stationary parts of Case I is shown in figure 10. In this case, the maximum pressure recovery of 0.53 occurs at the cross-over bend. Both *A* and *D* regions have the same pressure recovery around 0.15.
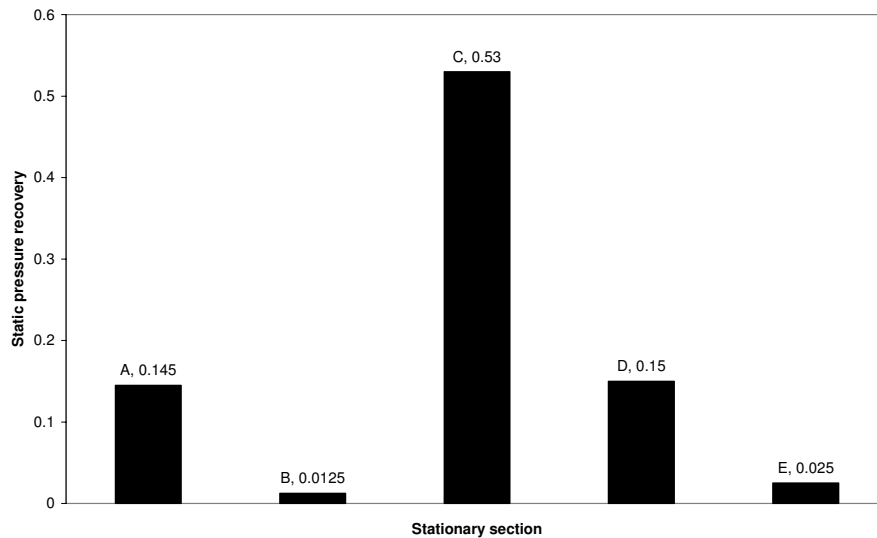
Figure 10. Static pressure recovery for stationary sections (Case I)

The loss coefficient for the stationary compartment is given by

$$\omega = \frac{P_{t2} - P_{t1}}{P_{t1} - P_{s1}} \tag{2}$$

It is shown that the diffuser and return channel are normally connected with the cross-over bend. In figure 11, the big losses may occur in this part because of the flow separation resulting from the strong meridional curvature and because of the long flow paths corresponding to the swirl velocity. The flow distortion at the exit of the cross-over bend and the large circumferential turning, that is required in the return channel, often result in the large losses, including the areas of separation flow, and the limit of the pressure that can be achieved in the return channel. This is probably due to the flow disturbance caused by the 90 degree change of direction of the airflow. The comparison for two cases is listed in Table 3, for Case I the maximum loss occurs at the cross-over bend whilst moves downstream to the return channel for Case II, it is because of severe flow blockage.
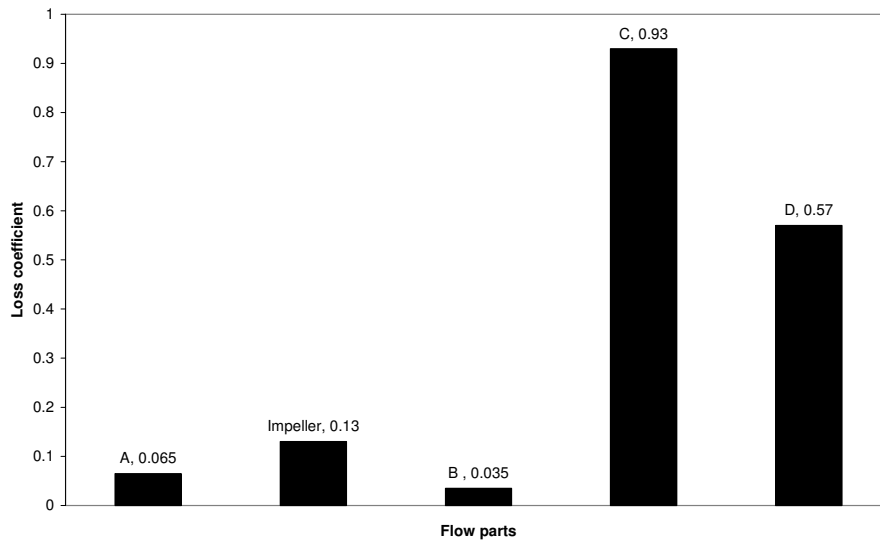
Figure 11. Distribution of total pressure loss along the centrifugal fan (Case I)

Section	Case I	Case II
A	0.065	0.50
Impeller	0.13	0.14
B	0.035	0.79
C	0.93	0.79
D	0.57	0.97

Table 3. Comparison of loss distribution of the centrifugal fan components

Total-to-total efficiency for the impeller is defined as

$$\eta = \frac{\left(\frac{P_{t2}}{P_{t1}}\right)^{\frac{\gamma-1}{\gamma}} - 1}{\frac{T_{t2}}{T_{t1}} - 1} \tag{3}$$

Considering the viscous effect to the total pressure rise, the total pressure coefficient can be expressed as

$$\pi = \tau^{\frac{\gamma-1}{\gamma}} \exp\left(\frac{-\Delta s}{R}\right) \tag{4}$$

where $\tau = 1 + \frac{U_2 C_{\theta 2}}{C_p T_{t1}}$, U_2 is the rotating velocity at impeller exit, $C_{\theta 2}$ is the circumferential component of absolute velocity at impeller exit, T_{t1} is the total temperature at impeller inlet. Δs is the entropy increment and R is the gas constant. The calculated overall performances for both cases are listed in Table 4. It is found that the total efficiency has 1% drop in presence of tip clearance. Meanwhile both the total-total pressure ratio and temperature ratio is drop too.

	Case I	Case II
η (total-total efficiency)	0.87	0.86
π (total-total pressure ratio)	1.15	1.12
τ (total temperature ratio)	1.065	1.057

Table 4. Comparison of overall performance between Case I and Case II

It is well known that the tip clearance influences static pressure rise and efficiency. By using a numerical model only with impeller, Eum & Kang [7] proposed an empirical relation of variation of total pressure rise and total efficiency with the tip clearance. With the existence of tip clearance, they concluded that the variation of total pressure rise and total-to-total efficiency were approximated as $\frac{\Delta \pi}{\pi^*} \approx 0.88 \frac{t}{b_2}$ and $\frac{\Delta \eta}{\eta^*} \approx 0.35 \frac{t}{b_2}$. In our study, the similarity with Eum's empirical model is the existence of tip clearance in the impeller, however, the inlet duct and outlet duct, the cross-over bend and return channel are additionally involved in our numerical model. In our case, it can be assessed that the coefficients are 0.20 and 0.08 for variations of total pressure and total efficiency, respectively, which is roughly 25% of the coefficients in the empirical model above.

4.2 Flow Restrictions

For an air delivery system, the pressure rise produced by impeller can be assumed to be balanced with the pressure drops in order to support fluid against the pressure gradients in the downstream components: diffuser, cross-over bend and return channel. The pressure characteristics of flow restrictions in a fan system can be commonly expressed mathematically through use of the polynomial expression,

$$\Psi = K\Phi^2 \tag{5}$$

where $\Psi = \frac{\Delta P}{\frac{1}{2}\rho U^2}$ the non-dimensional pressure rise coefficient, $\Phi = \frac{C_a}{U}$ the non-dimensional flow coefficient, C_a the axial velocity, K the constant of flow restriction and U the rotating velocity at impeller outlet section. For the centrifugal fan we studied, one can determine the constant K for two cases with the data in Table 4 and the given air flow rate. The constant K for the case with/without tip clearances is 4 and 5, respectively.
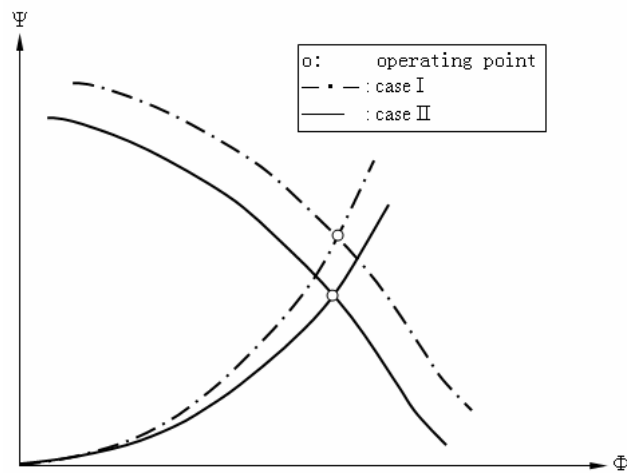
Figure 12. Schematic of flow restriction of the centrifugal fan system

Figure 12 shows the quantitatively view of the flow restriction for Case I and II. The parabola curves are flow restrictions for flow system related with flow blockage, wall frictions and swirling flow. The smaller the constant of parabola means the higher flow restriction. The intersection point, i.e., the balance point for the system, is for the point while the fan system is operating at. It is presumably the tip clearance increases the flow restriction coefficient, subsequently reduces the pressure rise at the same air flow rate. It can be concluded that keeping the same flow rate results in the total pressure drop in the presence of tip clearance, in turn, the flow rate will be reduced accordingly with the same total pressure.

5. Concluding remarks

In this paper, a centrifugal fan with high speed and compact dimension was chosen to study numerically and experimentally. There exists a tip clearance of 0.7 mm between the shrouded impeller rotating at 34,000 rpm and the fixed outer casing. The computational models with/without tip clearance were set up and the $k - \omega$ SST turbulence model and hybrid mesh were applied for unsteady solutions. The pressure rise of the centrifugal fan and the air flow rate were measured with a test bench. The effects of tip clearance on calculated flow field and loss generation were qualitatively analyzed and the comparison of fan performance between the prediction and measurement was shown in a favorable tendency. In terms of the flow restriction obtained for the centrifugal fan system, a new empirical constant accounting for the effects of tip clearance on flow restriction of the centrifugal fan system was approximated. In presence of the tip clearance, due to the difference of static pressure, the returned flow appears inside the clearance and re-circulates to the main stream near the impeller inlet, subsequently generating a stagnation point and changing the incidence angle and flow performance as well. The pressure loss is induced and the flow restriction is enhanced by the leakage flow through the clearance.

H. Krain. Review of centrifugal compressor's application and development. *Transaction of the ASME Journal of Turbomachinery, Vol. 127, Jan., 25-34*, 2005.

T. Meakhail. A study of impeller-diffuser-volute interaction in a centrifugal fan. *Transaction of the ASME Journal of Turbomachinery, Vol.127, Jan., 84-90*, 2005.

S. Khelladi, S. Kouidri, F. Bakir, and R. Rey. Flow study in the impeller-diffuser interface of a vaned centrifugal fan. *Journal of Fluid Engineering, Vol. 127, pp. 495-502*, 2005.

S. Khelladi, S. Kouidri, F. Bakir, and R. Rey. A numerical study on the aeroacoustics of a vaned centrifugal fan. *ASME Heat Transfer/Fluids Engineering Summer Conference, Houston, Texas, FEDSM2005-77134*, 2005.

A. Veress and R. Braembussche. Inverse design and optimization of a return channel for a multistage centrifugal compressor. *Transaction of the ASME Journal of Fluids Engineering, Vol. 126, Sept. 799-806*, 2004.

M. Ishida and T. Surana. Suppression of unstable flow at small flow rates in a centrifugal fan by controlling tip leakage flow and reverse flow. *Transaction of the ASME Journal of Turbomachinery, Vol. 127, Jan., 76-83*, 2005.

H.-J. Eum and S.-H. Kang. Numerical study on tip clearance effect on performance of a centrifugal compressor. *Proceedings of ASME FEDSM'02, Montreal, Quebec, Canada, July 14-18*, 2002.

K.-Y. Kim and S.-J. Seo. Shape optimization of forward-curved-blade centrifugal fan with navier-stokes analysis. *Transaction of the ASME Journal of Fluids Engineering, Vol. 126, Sept., 735-742*, 2004.

M. Zangeneh and M. Schleer. Investigation of an inversely designed centrifugal compressor stage-part i: Design and numerical verification. *Transaction of the ASME Journal of Turbomachinery, Vol. 126, Jan., 73-81*, 2004.

M. Schleer and S.-S. Hong. Investigation of an inversely designed centrifugal compressor stage-part ii: Experimental investigations. *Transaction of the ASME Journal of Turbomachinery, Vol. 126, JANUARY 2004, 82-90*, 2004.

Y.-J. Moon, Y. Cho, and H.-S. Nam. Computation of unsteady viscous flow and aeroacoustic noise of cross flow fans. *Computers & Fluids, Vol. 32, 995-1015*, 2003.

S.-J. Seo, K.-Y. Kim, and S.-H. Kang. Calculations of three-dimensional viscous flow in a multiblade centrifugal fan by modeling blade forces. *Proceedings of Inst. Mech. Eng. Part A: J. Power and Energy, Vol. 217, 287-297*, 2003.

A. Lazzaretto. A criterion to define cross-flow fan design parameters. *Journal of Fluids Engineering, Vol.125, 680-683*, 2003.

A. Lazzaretto, A. Toffolo, and A. D. Martegani. A systematic experimental approach to cross-flow fan design. *Transaction of the ASME Journal of Fluids Engineering, Vol. 125, July, 684, 693*, 2003.

A. Toffolo. On cross-flow fan theoretical performance and efficiency curves: An energy loss analysis on experimental data. *Transaction of the ASME Journal of Fluids Engineering, Vol. 126, Sept., 743-751*, 2004.

FLUENT. Fluent, inc. 1998.

F.R. Menter. Zonal two equation $k - \omega$ turbulence models for aerodynamic flows. *AIAA Paper 93-2906*, 1993.

J.E. Bardina, P.G. Huang, and T.J. Coakley. Turbulence modeling, validation, testing and development. *NASA Technical Memorandum 110446*, 1997.